Available online at www.sciencedirect.com
ScienceDirect
Trans. Nonferrous Met. Soc. China 26(2016) 1301−1309
Transactions of Nonferrous Metals Society of China
www.tnmsc.cn

Dynamic spheroidization kinetics behavior of Ti−6.5Al−2Zr−1Mo−1V alloy with lamellar microstructure

Xian-juan DONG[1,2], Shi-qiang LU[2], Hai-zhong ZHENG[3]

1. Aeronautical Science and Technology Key Laboratory of Aeronautical Materials Hot Processing Technology, Nanchang Hangkong University, Nanchang 330063, China;
2. Institute of Aeronautic and Manufacturing Engineering, Nanchang Hangkong University, Nanchang 330063, China;
3. Institute of Materials Science and Engineering, Nanchang Hangkong University, Nanchang 330063, China

Received 24 June 2015; accepted 3 March 2016

Abstract: The dynamic spheroidization kinetics behavior of Ti−6.5Al−2Zr−1Mo−1V alloy with a lamellar initial microstructure was studied by isothermal hot compression tests in the temperature range of 750−950 ℃ and strain rates of 0.001−10 s^{-1}. The results show that the spheroidized fraction of alpha lamellae increases with the increase of temperature and the decrease of strain rate. The spheroidization kinetics curves predicted by JMAK equation agree well with experimental ones. The corresponding SEM and TEM observations indicate that the dynamic spheroidization process can be divided into two stages. The primary stage is boundary splitting formed by two competing mechanisms which are dynamic recrystallization and mechanical twin. In the second stage, the penetration of beta phase into the alpha/alpha grain boundaries is dominant, which is controlled in nature by diffusion of the chemical elements such as Al, Mo and V.

Key words: titanium alloy; lamellar microstructure; spheroidization; kinetics equation

1 Introduction

The near alpha titanium alloy Ti−6.5Al−2Zr−1Mo−1V is extensively used in aerospace application. It can work at about 500 ℃ and is the general alloy of bar stock and sheet material. Because of the allotropic transformation, this alloy can acquire a large variety of microstructures with different alpha morphologies depending on thermomechanical processing, such as lamellar, equiaxed and duplex microstructure. The conversion of lamellar microstructure to equiaxed microstructure, called spheroidization, is the most important in the hot working procedure. It is worth noting that the lamellar microstructures have preferable high-temperature stability and cannot be converted to equiaxed microstructures only through heat treatment. Consequently, large plastic deformation in alpha and beta phases field is essential.

WEISS et al [1,2] proposed that spheroidization can accomplish by the formation of low and high angle alpha/alpha boundaries or shear bands, followed by penetration of beta phase to complete the separation. SESHACHARYULU et al [3−5] considered that spheroidization process may also be regarded as a type of dynamic recrystallization since it involves two competitive processes, namely rate of nucleation and rate of migration. SEMIATIN et al [6−8] have performed a great deal of research on the spheroidization kinetics behavior of Ti−6Al−4V titanium alloy. They have assumed that the development of sub-boundaries within alpha lamellae and dynamic coarsening process together control the rate of dynamic spheroidization. More recently, the kinetics of dynamic spheroidization in titanium alloy with a lamellar microstructure has been reported by many scholars [9−11]. Some of them are Ti−6.5Al−2Zr−1Mo−1V alloy [12−14].

The objective of this work is to research the dynamic spheroidization kinetics behavior and clarify the deformation mechanism during hot forging. For this purpose, isothermal constant strain rate compression experiments and corresponding microstructure

Foundation item: Project (2014ZE56015) supported by Aeronautical Science Foundation of China; Project (51261020) supported by the National Natural Science Foundation of China; Project (Zk201001004) supported by the Open Fund of the Aeronautical Science and Technology Key Laboratory of Aeronautical Material Hot Processing Technology, China

Corresponding author: Shi-qiang LU; Tel: +86-791-83863039; Fax: +86-791-83863039; E-mail: niatlusq@126.com

DOI: 10.1016/S1003-6326(16)64233-4

examination of Ti−6.5Al−2Zr−1Mo−1V alloy with a lamellar initial microstructure were conducted in wide ranges of temperature and strain rate to model the dynamic spheroidization kinetics process. This study may provide important theory foundation on designing processing techniques and controlling microstructure evolution.

2 Experimental

The material used in the present investigation has the following chemical composition (mass fraction, %): Al 6.3, Zr 1.97, Mo 1.4, V 1.4, O 0.08, N 0.01, Ti balance. The beta transus temperature for the material is approximately 990 ℃. The raw material was beta solution treated at 1020 ℃ for 30 min and then air cooled to obtain lamellar microstructure with prior beta grains of about 450 μm and lamellar alpha thickness of 1 μm (Fig. 1).

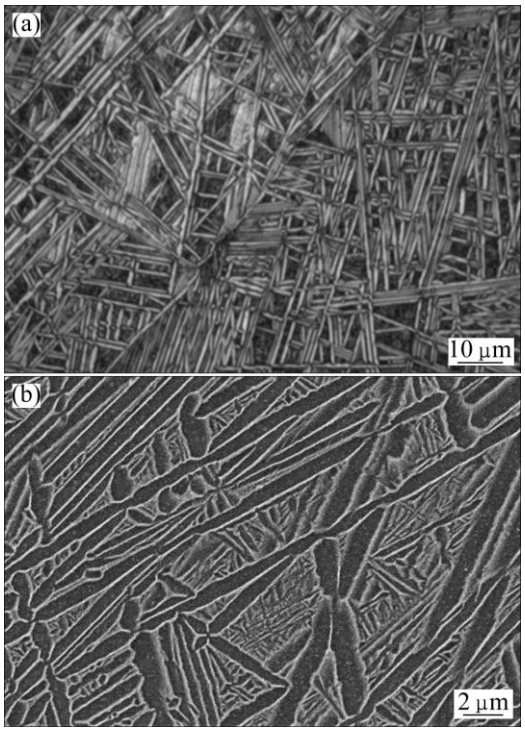

Fig. 1 Initial microstructures of Ti−6.5Al−2Zr−1Mo−1V alloy: (a) OM; (b) SEM

The isothermal constant strain rate compression experiments were carried out by THERMECMASTOR-Z thermal simulation machine. Cylinder specimens of 8 mm in diameter and 12 mm in length were machined with grooves of 0.2 mm in depth at both end faces to store glass power lubricant for reducing friction. The specimens were heated to test temperature at a heating rate of 10 ℃/s by vacuum induction heating, held for 210 s and compressed to the corresponding reduction, followed by helium gas cooling to preserve the hot deformed microstructure. The 50% height reduction tests were performed at the temperatures of 750, 800, 850, 900 and 950 ℃ and the strain rates of 0.001, 0.01, 0.1, 1 and 10 s^{-1}. Other compressive tests with different height reductions (3%, 5%, 8%, 13%, 20%, 30%, 40%, 60% and 70%) were carried out at the temperatures of 850 ℃ and 900 ℃ to obtain the spheroidization kinetics curves.

After the hot deformation, the compressed specimens were sectioned parallel to the compression axis by wire cutting for microstructure observation. The metallographic samples were polished mechanically and etched with a Kroll reagent of 2% HF, 4% HNO_3 and 94% H_2O. All micrographs were taken from the large deformation zone of the compressed samples on a XJP−6A type microscope and estimated using quantitative metallography analysis software. Spheroidization was considered to be alpha phase morphology with a aspect ratio (the ratio of length to width) less than 3.

3 Results and discussion

3.1 Effects of hot deformation parameters on spheroidization

The optical micrographs of Ti−6.5Al−2Zr−1Mo−1V alloy at the true strain of 0.69 are presented in Fig. 2. It is suggested that the strain rate and temperature both have obvious effects on dynamic spheroidization. The spheroidized fraction increases with strain rate decreasing and temperature increasing. The initial positions of dynamic spheroidization occur at or near the prior beta grain boundaries (PBGD) and at kinks of the alpha colonies, as the white arrows shown in Fig. 2. Dynamic spheroidization within these two regions is probably favored because of the deformation incompatibilities between the prior beta grain boundary and colony alpha phase [6].

Figure 3 shows the influence curves of strain rate and temperature on the spheroidized fraction of alpha lamellae at the true strain of 0.69. In Fig. 3(a), the spheroidized fraction of alpha lamellae decreases with the strain rate increasing. But it is worth noting that the effect is more significant at 0.001−0.1 s^{-1} than at 0.1−10 s^{-1}. This is because dynamic spheroidization is a thermal activation process. At low temperatures or at high strain rates, the diffusion rate is slow and the diffusion time is insufficient. In Fig. 3(b) the slope of line increases with decreasing strain rate at 10−0.1 s^{-1} and is basically the same at strain rates of 0.1 and 0.01 s^{-1}, and then it has a slightly decline at 0.001 s^{-1}. These phenomena may be ascribed to the coarsening of

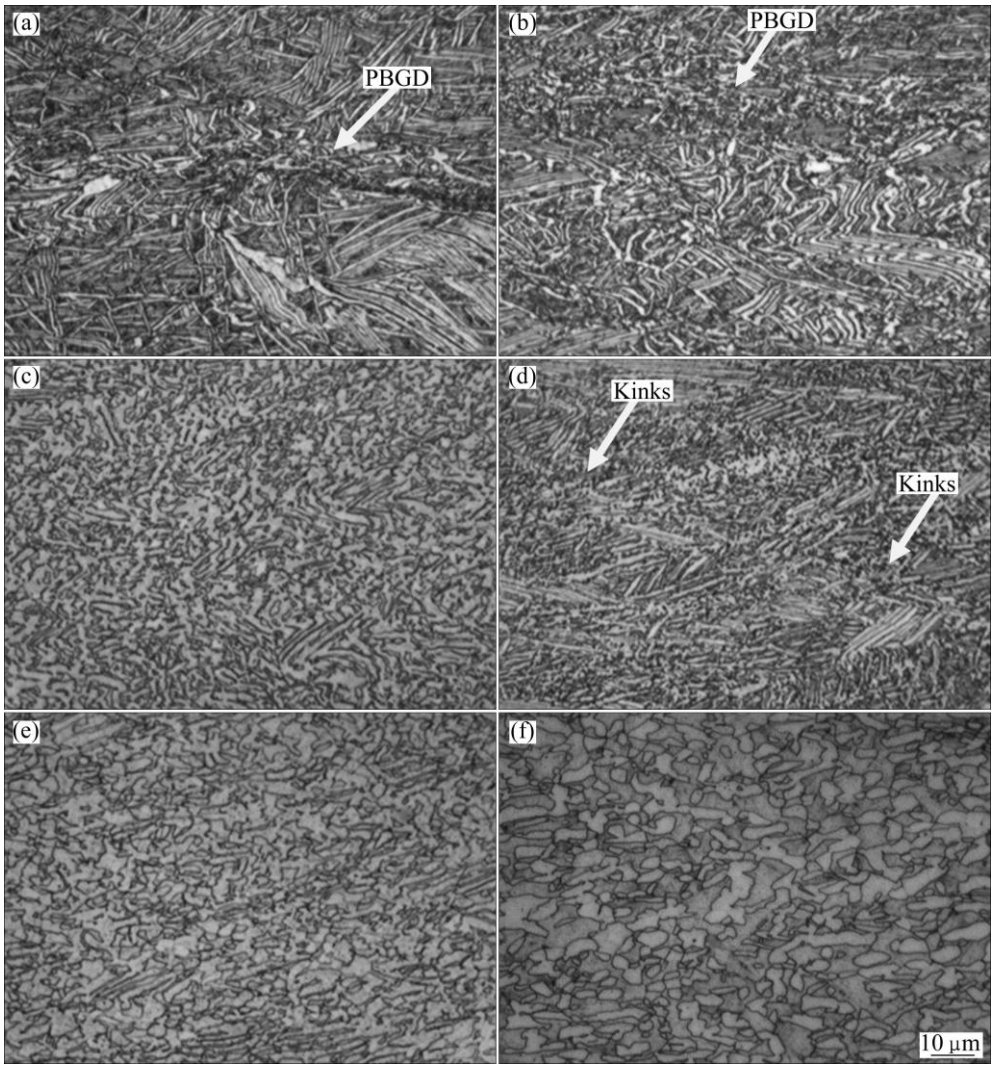

Fig. 2 Microstructures of Ti−6.5Al−2Zr−1Mo−1V alloy deformed at true strain of 0.69: (a) 850 ℃, 10 s^{-1}; (b) 850 ℃, 0.1 s^{-1}; (c) 850 ℃, 0.001 s^{-1}; (d) 750 ℃, 0.001 s^{-1}; (e) 900 ℃, 0.001 s^{-1}; (f) 950 ℃, 0.001 s^{-1} (compression direction is perpendicular to horizontal axis)

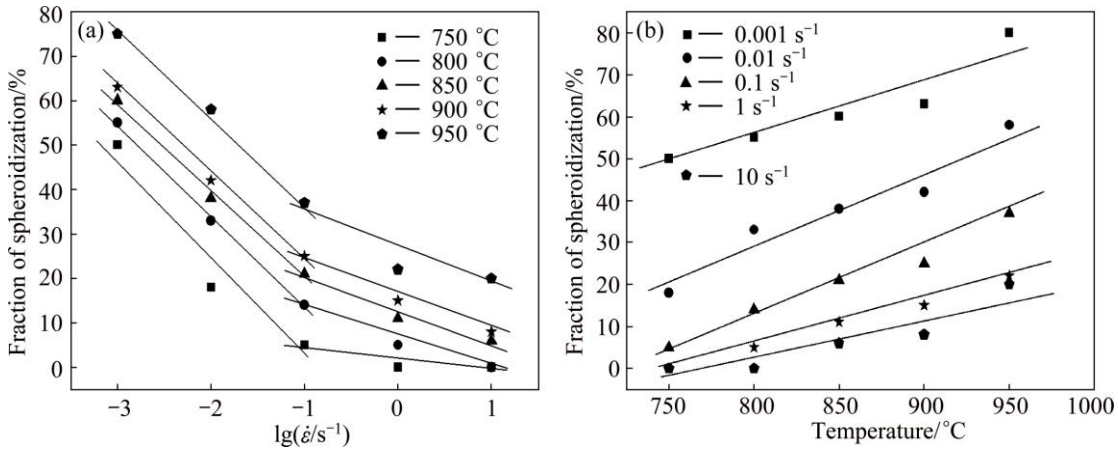

Fig. 3 Dependence of spheroidized fraction at true strain of 0.69 on strain rate (a) and temperature (b)

alpha grains at low strain rates (0.01 and 0.001 s^{-1}), as shown in Fig. 4. The thickness of alpha lamellae and the diameter of the spheroidized alpha grains both exhibit a strong dependence on temperature at strain rates of 0.01 and 0.001 s^{-1}, and the grain growth rate of 0.001 s^{-1} is significantly larger than that of 0.01 s^{-1}. The higher the temperature and the lower the strain rate are, the larger the lamellar and spheroidized alpha grains grow. PARK

et al [15] found that the flow behavior of Ti−6.5Al−2Sn−4Zr−2Mo−0.1Si alloy showed a noticeable dependence on strain rate due to the competition between dynamic spheroidization and dynamic coarsening. As illustrated in Figs. 2(c), (e) and (f), the growth of alpha grains results in the reducing of alpha/beta grains interface. The coarsening rate of alpha grains further increases because the migration rate in homophase boundaries is higher than that in heterophase boundaries [16,17]. Compared with low strain rates (0.01 and 0.001 s^{-1}), the thickness of alpha lamellae remains the same with the initial microstructure at strain rates of 0.1−10 s^{-1}. SHELL et al [6] showed that the spheroidized rate of alpha lamellae was the most rapid for the thinnest alpha platelet among three transformed beta microstructures of 0.25, 3 and 5 μm-thick alpha laths. Thus, spheroidization rate in Fig. 3(b) decreases at strain rates of 0.001 and 0.01 s^{-1}.

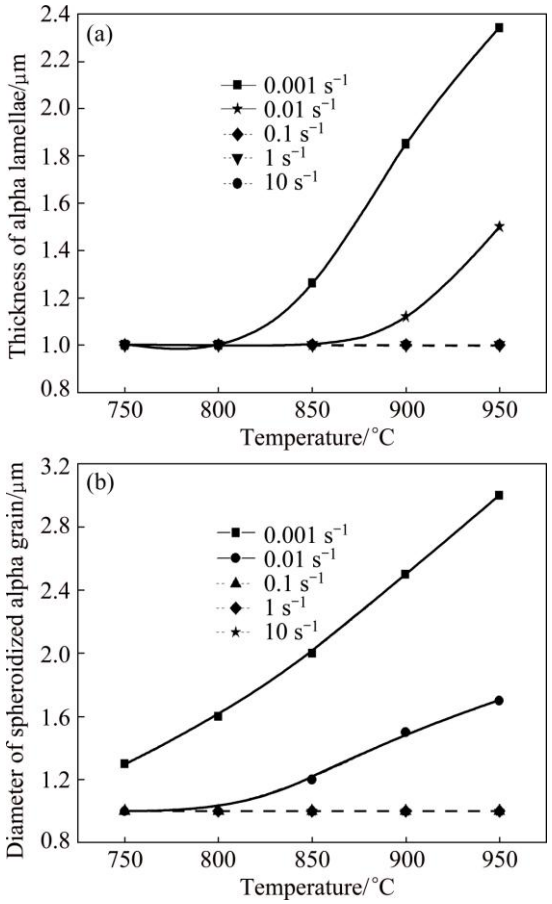

Fig. 4 Alpha grain size as function of deformation temperature at true strain of 0.69: (a) Thickness of alpha lamellae; (b) Diameter of spheroidized alpha grain

Figure 5 shows the microstructures of Ti−6.5Al−2Zr−1Mo−1V alloy with various strains at 900 ℃ and 0.01 s^{-1}. It can be seen that the degree of spheroidization increases with the increase of true strain. During hot deformation, the alpha lamellae paralleled to the compression axis kink considerably and lamellae in other orientations rotate gradually to the direction perpendicular to compression axis. Ultimately, all alpha lamellae have distributed along the horizontal direction. With increase in true strain to 0.69 (Fig. 5(d), it is difficult to distinguish the primary beta grain boundaries from the alpha lamellae. Even at the true strain as large as 1.20 (Fig. 5(f), there are a large number of alpha lamellae distributed along the horizontal direction with high aspect ratio.

3.2 Dynamic spheroidization kinetics behavior

Typical spheroidization kinetics curves obtained at deformation temperatures of 850 ℃ and 900 ℃ are plotted in Fig. 6. It clearly demonstrates a typical sigmoid type. At first they have a gestation period, and then the spheroidized fraction increases rapidly with the true strain. As the true strain approximately achieves 1.0, the rates of the curves decrease obviously with the true strain. This may attribute to the coarsening of the alpha lamellae at high deformation temperature (Fig. 4(a)). Figure 6 shows that the critical strain for initiation spheroidization of Ti−6.5Al−2Zr−1Mo−1V alloy is in the range of 0.20−0.40 which decreases with temperature increasing and strain rate decreasing. This is due to that the spheroidization of the alpha lamellae is a thermally activated process with the diffusion of alloy elements at the alpha/beta interface [18,19].

It is assumed that the dynamic spheroidized fraction (f_s) followed the JMAK type as Eq. (1):

$$f_s=1-\exp(-kt^n) \tag{1}$$

where f_s is the volume fraction of dynamic spheroidized alpha lamellae, t is the deformation time of dynamic spheroidization [$t=(\varepsilon-\varepsilon_c)/\dot{\varepsilon}$], ε is the true strain, $\dot{\varepsilon}$ is the strain rate, ε_c is the critical strain for initiation of dynamic spheroidization.

Taking natural logarithm to Eq. (1) on both sides, we can obtain

$$\ln\left[\ln\left(\frac{1}{1-f_s}\right)\right]=\ln k+n\ln\left(\frac{\varepsilon-\varepsilon_c}{\dot{\varepsilon}}\right) \tag{2}$$

Put the experimental data into Eq. (2), it is found that there has a good linear relationship between $\ln\{\ln[1/(1-f_s)]\}$ and $\ln[(\varepsilon-\varepsilon_c)/\dot{\varepsilon}]$, in which k and n are fitting constants.

There is an empirical formula expressed as

$$Z=A\exp(B\varepsilon_c) \tag{3}$$

where A and B are constants.

With the calculation of experimental values, the logarithm of Zener−Hollomon parameter (also called temperature compensated strain rate parameter, Z) is linear with the critical strain for initiation spheroidization in Fig. 6. Then, the relationship between Zener−

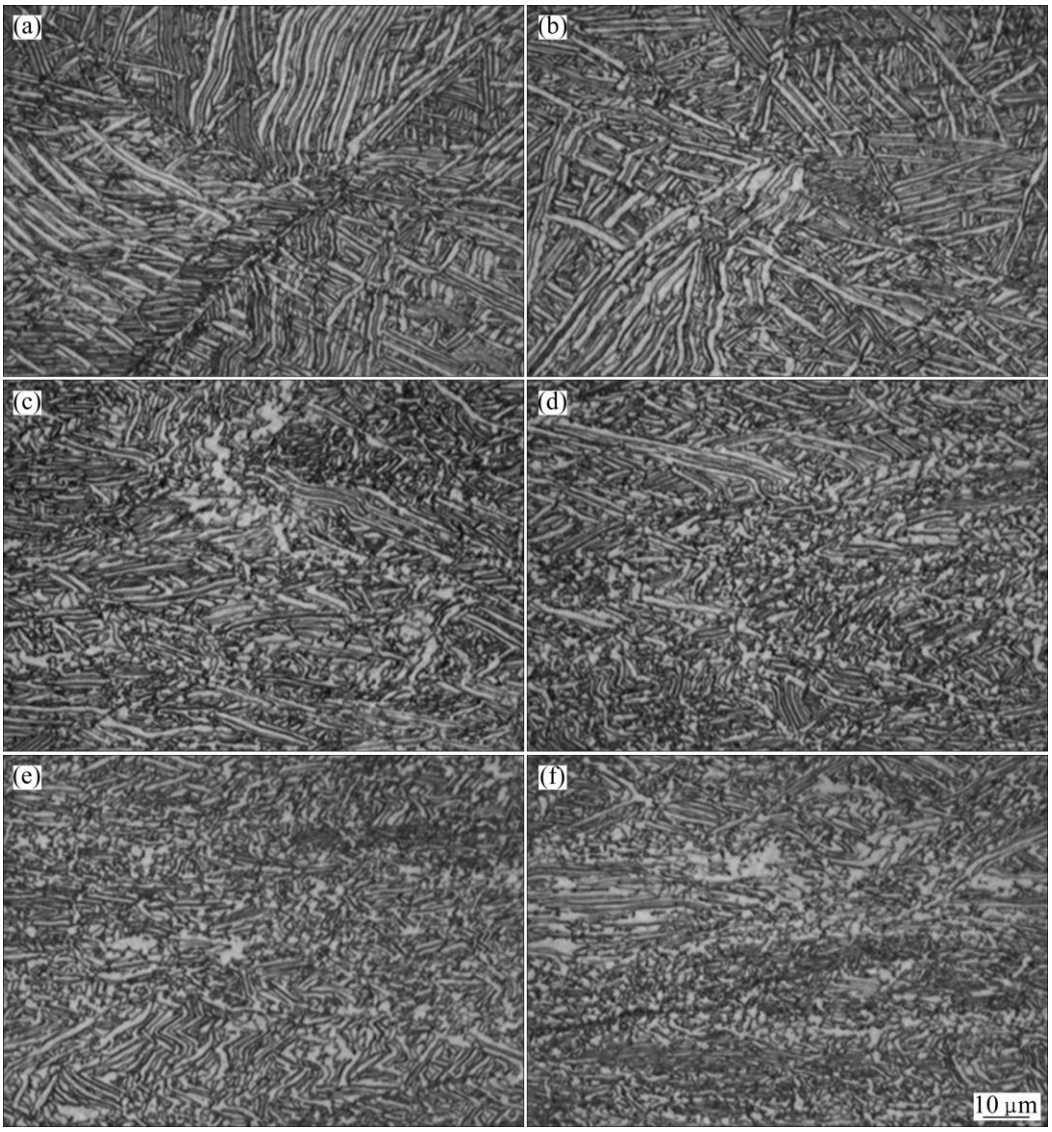

Fig. 5 Microstructures of Ti−6.5Al−2Zr−1Mo−1V alloy deformed at 900 ℃ and 0.01 s^{-1} with true strains of 0.14 (a), 0.22 (b), 0.36 (c), 0.69 (d), 0.92 (e) and 1.20 (f) (Compression direction is perpendicular to horizontal axis)

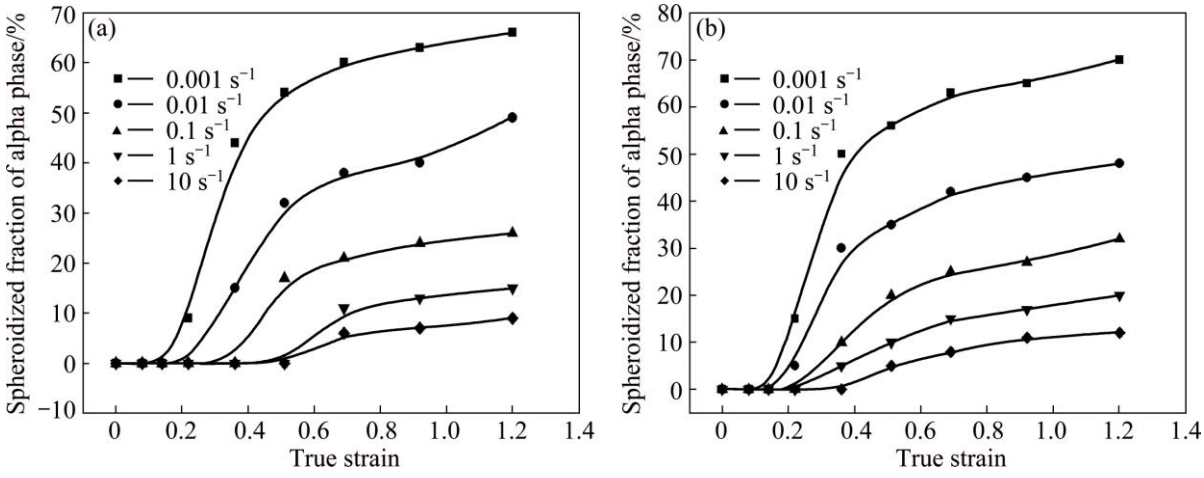

Fig. 6 Spheroidized fraction of Ti−6.5Al−2Zr−1Mo−1V alloy as function of true strain and strain rate at temperatures of 850 ℃ (a) and 900 ℃ (b)

Hollomon parameter and critical strain ε_c can be expressed as follows:

$$\varepsilon_c = \frac{\ln Z - 51.322}{29.707} \tag{4}$$

Thus, the spheroidization kinetics of the alpha lamellae in Ti−6.5Al−2Zr−1Mo−1V alloy can be described as

$$f_s = 1 - \exp\left\{-0.202\left[\frac{\varepsilon - \left(\frac{\ln Z - 51.322}{29.707}\right)}{\dot{\varepsilon}}\right]^{0.253}\right\} \tag{5}$$

in which Z is given by the Arrhenius equation:

$$Z = \dot{\varepsilon}\exp\left(\frac{6.17\times10^5}{8.314T}\right) \tag{6}$$

where T is the thermodynamic temperature.

The calculated spheroidization kinetics curves are shown in Fig. 7. The average error of experimental and calculated values is 9.59%. This indicates that the calculated values agree well with the experimental ones.

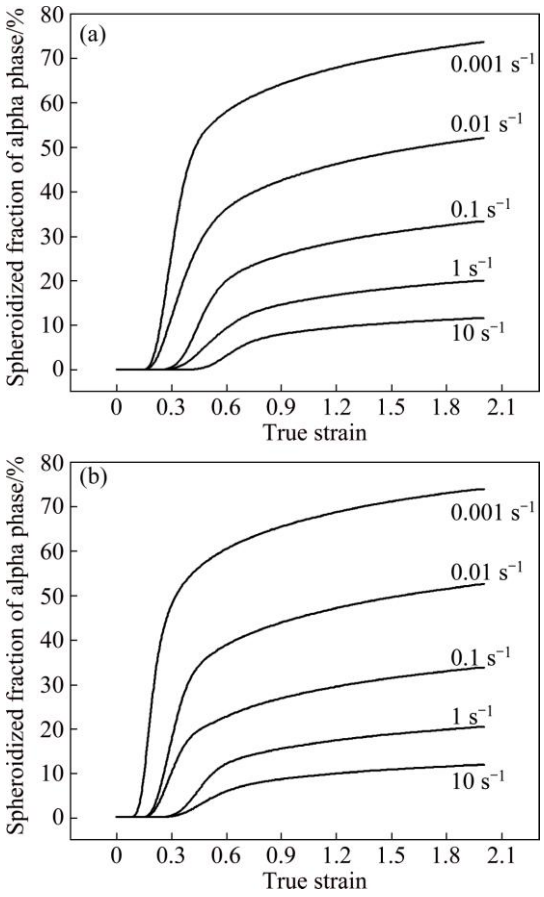

Fig. 7 Calculated spheroidization kinetics curves of Ti−6.5Al−2Zr−1Mo−1V alloy at temperatures of 850 ℃ (a) and 900 ℃ (b)

This further demonstrates that the spheroidization kinetics equation developed in this study can accurately predict the spheroidization fraction as functions with the strain, strain rate and temperature.

3.3 Mechanism of dynamic spheroidization

Figure 8 illustrates the SEM images of Ti−6.5Al−2Zr−1Mo−1V alloy deformed at 850 ℃ and 0.01 s^{-1} to a true strain of 0.69. As the white arrows shown, the fragmentation and spheroidization of alpha lamellae firstly appear at the boundaries of the primary beta grains and the regions near different oriented colony boundaries, where deformation easily happens. This is because the alpha colony with the same alpha lamellar orientation deforms wholly as a grain group, causing the plastic deformation concentrate at the intersection of different orientation colonies.

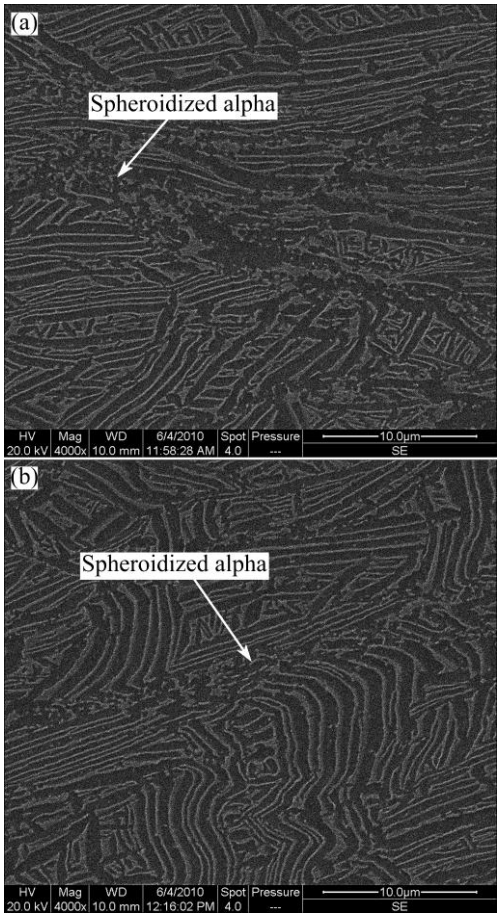

Fig. 8 SEM images of initial spheroidized positions of Ti−6.5Al−2Zr−1Mo−1V alloy deformed at 850 ℃ and 0.01 s^{-1} to true strain of 0.69 at boundary of primary beta grain (a) and region near colony boundaries (b)

Further TEM micrographic examination of Ti−6.5Al−2Zr−1Mo−1V alloy deformed to a true strain of 0.69 in Fig. 9 reveals that dynamic recrystallization and mechanical twin play important roles in the spheroidization of the alpha lamellae. As shown in

Fig. 9(a), sub-grains separate the alpha lamellae and mostly run through the width direction, which causes the grain sizes of the spheroidized alpha being similar to the alpha lamellar spacing. Subsequently, high angle grain boundaries come into being to complete the dynamic recrystallization. Such behavior is often associated with the continuous dynamic recrystallization (CDRX) [20]. CDRX may occur mainly at high temperatures (850−900 ℃) and low strain rates (0.001−0.1 s^{-1}). A number of mechanical twins are observed within the alpha lamellae in Fig. 9. They separate the long alpha lamellae into several short segments. The number of twins and the contribution of twinning to deformation increase with increasing strain rate and decreasing temperature. Mechanical twins usually appear at low temperatures (750−850 ℃) and high strain rates (0.1−10 s^{-1}). Reference [21] showed that twins and dislocation networks occurred in the Ti−6.5Al−3.5Mo−1.5Zr−0.3Si alloy with a Widmanstätten initial microstructure. WYATT et al [22] performed the deformation mechanisms and kinetics of time-dependent twinning in α-Ti−1.6V alloy at four strain rates of 10^{-1}, 10^{-2}, 10^{-1}, and 10^{-6} s^{-1}.

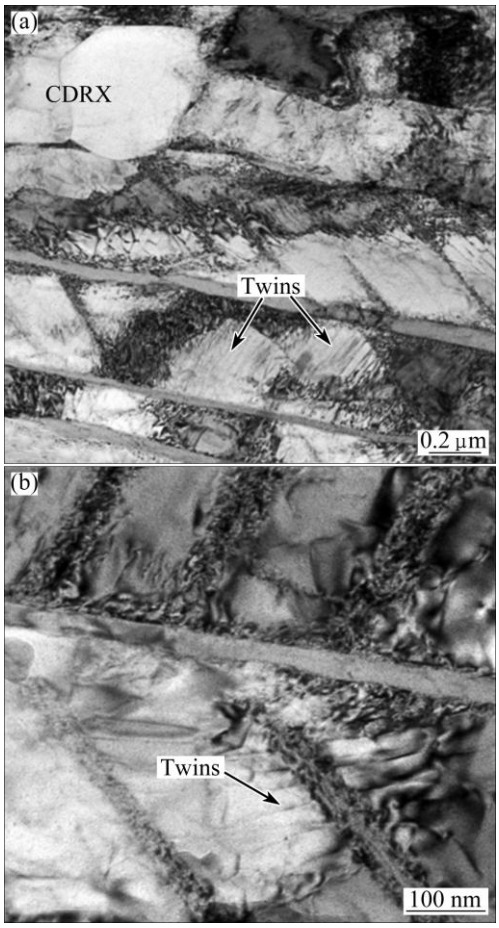

Fig. 9 TEM images of Ti−6.5Al−2Zr−1Mo−1V alloy deformed to true strain of 0.69 indicating boundary splitting at 850 ℃ and 0.1 s^{-1}

The EDS results were used to analyze the element contents in different regions at the interfaces of alpha and beta phases in Fig. 10 and Table 1. It is found that the dark gray alpha phase (Spectrum 4 in Fig. 10) is rich in Al (5.40%) compared with the light gray beta phase of 4.26% (Spectrum 1 in Fig. 10). The beta stable elements Mo and V are enriched in beta phases and diffuse along the interfaces of alpha and beta phases. This is because the arrangement of atoms at grain boundaries is irregular and the diffusion rate of alloy elements such as Al, Mo and V at grain boundaries is faster than those in interior of grains. Thus, "cups" penetrated by beta phase along the alpha/alpha grain boundaries are formed. They wedge the alpha/alpha boundaries formed by sub-boundaries and mechanical twins and separate the long alpha lamellae into several parts with short rod or elliptical shape which would spheroidize fully by the further migration of the alloy elements.

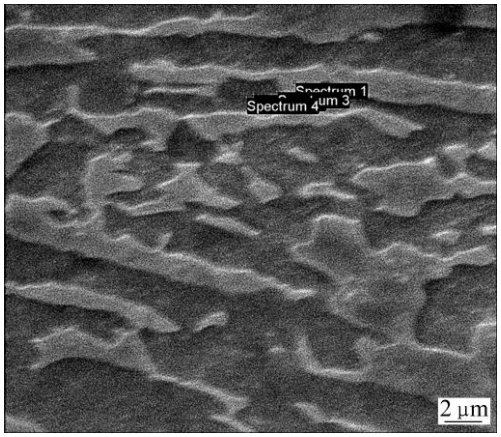

Fig. 10 SEM image of Ti−6.5Al−2Zr−1Mo−1V alloy deformed to true strain of 0.69 at 900 ℃ and 0.001 s^{-1}

Table 1 EDS results of spectra in Fig. 10

Spectrum	Mole fraction/%					
	Al	Ti	V	Zr	Mo	Total
Spectrum 1 (Beta phase)	4.26	87.46	3.48	2.51	2.29	100.00
Spectrum 3 (Interface)	4.27	89.95	2.50	1.90	1.38	100.00
Spectrum 4 (Alpha phase)	5.40	92.64		1.96		100.00

Obviously, the dynamic spheroidization process can be divided into two stages. One is controlled by boundary splitting which is associated with boundary formation by dynamic recrystallization or mechanical twin, the other is predominated by the penetration of beta phase into the alpha/alpha grain boundaries. In the first stage, the two mechanisms of dynamic recrystallization and mechanical twin compete and complement each other. With the decrease of deformation temperature and

increase of strain rate, mechanical twins may play a more important role owning to the decrease of dislocation slips. The second stage is essentially the diffusion of chemical elements such as Al, Mo and V. This is different with the view of Weiss's [1] which considered that alpha lamellae break-up is caused by sub-boundary formation or heavily localized shearing zones.

4 Conclusions

1) The dynamic spheroidized fraction of alpha lamellae increases with temperature increasing and strain rate decreasing. A critical strain for initiation of spheroidization is 0.20−0.40 which decreases with the decrease of strain rate and increase of temperature.

2) The spheroidization kinetics curve follows a typical sigmoid type. An Avrami type equation which agrees well with the experimental results is established to accurately predict the spheroidization kinetics behavior.

3) Boundary splitting and the penetration of beta phase are two main stages in the dynamic spheroidization process. In the first stage, dynamic recrystallization and mechanical twin compete with each other. In the second stage, beta phase wedges the alpha/alpha boundaries and separates the long alpha lamellae into several parts.

References

[1] WEISS I, FROES F H, EYLN D, WELSCH G E. Modification of alpha morphology in Ti−6Al−4V by thermomechanical processing [J]. Metallurgical Transactions A, 1986, 17: 1935−1947.

[2] WEISS I, SEMIATIN S L. Thermomechanical processing of alpha titanium alloys: An overview [J]. Materials Science and Engineering A, 1999, 263: 243−256.

[3] SESHACHARYULU T, MEDEIROS S C, MORGAN J T, MALAS J C, FRAZIER W G, PRASAD Y V R K. Hot deformation mechanisms in ELI grade Ti−6Al−4V [J]. Scripta Materialia, 1999, 41: 283−288.

[4] SESHACHARYULU T, MEDEIROS S C, MORGAN J T, MALAS J C, FRAZIER W G, PRASAD Y V R K. Hot deformation and microstructural damage mechanisms in extra-low interstitial (ELI) grade Ti−6Al−4V [J]. Materials Science and Engineering A, 2000, 279: 289−299.

[5] SESHACHARYULU T, MEDEIROS S C, FRAZIER W G, PRASAD Y V R K. Microstructural mechanisms during hot working of commercial grade Ti−6Al−4V with lamellar starting structure [J]. Materials Science and Engineering A, 2002, 325: 112−125.

[6] SHELL E B, SEMIATIN S L. Effect of initial microstructure on plastic flow and dynamic globularization during hot working of Ti−6Al−4V [J]. Metallurgical and Materials Transactions A, 1999, 30: 3219−3229.

[7] SEMIATIN S L, BIELER T R. The effect of alpha platelet thickness on plastic flow during hot working of Ti−6Al−4V with a transformed microstructure [J]. Acta Materialia, 2001, 49: 3565−3573.

[8] ZHEREBTSOV S, MURZINOVA M, SALISHCHEV G, SEMIATIN S L. Spheroidization of the lamellar microstructure in Ti−6Al−4V alloy during warm deformation and annealing [J]. Acta Materialia, 2011, 59: 4138−4150.

[9] LIU Jiang-lin, ZENG Wei-dong, LAI Yun-jin, JIA Zhi-qiang. Constitutive model of Ti17 titanium alloy with lamellar-type initial microstructure during hot deformation based on orthogonal analysis [J]. Materials Science and Engineering A, 2014, 597: 387−394.

[10] LI L, LUO J, YAN J J, LI M Q. Dynamic globularization and restoration mechanism of Ti−5Al−2Sn−2Zr−4Mo−4Cr alloy during isothermal compression [J]. Journal of Alloys and Compounds, 2015, 622: 174−183.

[11] YE Xiao-xin, TSE ZIONTH T H, TANG Guo-yi, GENG Yu-bo, SONG Guo-lin. Influence of electropulsing globularization on the microstructure and mechanical properties of Ti−6Al−4V alloy strip with lamellar microstructure [J]. Materials Science and Engineering A, 2015, 622: 1−6.

[12] GAO Peng-fei, YANG He, FAN Xiao-guang, ZHU Shuai. Unified modeling of flow softening and globularization for hot working of two-phase titanium alloy with a lamellar colony microstructure [J]. Journal of Alloys and Compounds, 2014, 600: 78−83.

[13] FAN X G, YANG H, YAN S L, GAO P F, ZHOU J H. Mechanism and kinetics of static globularization in TA15 titanium alloy with transformed structure [J]. Journal of Alloys and Compounds, 2012, 533: 1−8.

[14] WU Cheng-bao, YANG He, FAN Xiao-guang, SUN Zhi-chao. Dynamic globularization kinetics during hot working of TA15 titanium alloy with colony microstructure [J]. Transactions of Nonferrous Metals Society of China, 2011, 21(9): 1963−1969.

[15] PARK C H, LEE B, SEMIATIN S L, LEE C S. Low-temperature superplasticity and coarsening behavior of Ti−6Al−2Sn−4Zr−2Mo−0.1Si [J]. Materials Science and Engineering A, 2010, 527: 5203−5211.

[16] SABY M, MASSONI E, BOZZOLO N. A metallurgical approach to individually assess the rheology of alpha and beta phases of Ti−6Al−4V in the two-phase domain [J]. Materials Charactterization, 2014, 89: 88−92.

[17] SHARMA G, RAMANUJAN R V, TIWARI G P. Instability mechanisms in lamellar microstructures [J]. Acta Materialia, 2000, 48: 875−889.

[18] SEMIATIN S L, SEETHARAMAN V, WEISS I. Flow behavior and globularization kinetics during hot working of Ti−6Al−4V with a colony alpha microstructure [J]. Materials Science and Engineering A, 1999, 263: 257−271.

[19] WANG Kai-xuan, ZENG Wei-dong, ZHAO Yong-qing, LAI Yun-jin, ZHOU Yi-gang. Dynamic globularization kinetics during hot working of Ti−17 alloy with initial lamellar microstructure [J]. Materials Science and Engineering A, 2010, 527: 2559−2566.

[20] ZHEREBTSOV S, MURZINOVA M, SALISHCHEV G, SEMIATIN S L. Spheroidization of the lamellar microstructure in Ti−6Al−4V alloy during warm deformation and annealing [J]. Acta Materialia, 2011, 59: 4138−4150.

[21] HUANG L J, GENG L, LI A B, WANG G S, CUI X P. Effects of hot compression and heat treatment on the microstructure and tensile property of Ti−6.5Al−3.5Mo−1.5Zr−0.3Si alloy [J]. Materials Science and Engineering A, 2008, 489: 330−336.

[22] WYATT Z W, JOOST W J, ZHU D, ANKEM S. Deformation mechanisms and kinetics of time-dependent twinning in an α-titanium alloy [J]. International Journal of Plasticity, 2012, 39: 119−131.

层片组织 Ti−6.5Al−2Zr−1Mo−1V 合金动态等轴化动力学行为

董显娟[1,2]，鲁世强[2]，郑海忠[3]

1. 南昌航空大学 航空材料热加工技术航空科技重点实验室，南昌 330063；
2. 南昌航空大学 航空制造工程学院，南昌 330063；
3. 南昌航空大学 材料科学与工程学院，南昌 330063

摘 要：通过等温热压缩实验研究 Ti−6.5Al−2Zr−1Mo−1V 合金在温度 750~950 ℃、应变速率 0.001~10 s^{-1} 条件下的动态等轴化动力学行为。结果表明，层片组织 α 相的等轴化分数随变形温度升高和应变速率降低而增大，并构建了 JMAK 型等轴化动力学方程，且方程预测的等轴化动力学曲线与实验值吻合较好。此外，结合 SEM 和 TEM 微观组织观察发现，层片组织 α 相的动态等轴化过程分为两个阶段，首先是由动态再结晶和机械孪晶两个互相竞争的机制引起的晶界分离阶段；第二阶段中 β 相渗入 α/α 界面导致等轴化完成，β 相渗入 α/α 界面实质上是由 Al、Mo 和 V 等合金元素的扩散造成的。

关键词：钛合金；层片组织；等轴化；动力学方程

(Edited by Xiang-qun LI)